

Article

Monitoring of Structures by a Laser Pointer: Dynamic Measurement of Displacements of a Bridge

Serena Artese ^{1,*}, Vladimiro Achilli ² and Raffaele Zinno ³

¹ Dept. of Civil Engineering, University of Calabria, Via Bucci cubo 45B, 87036 Rende, Italy; E-Mail:

serena.artese@unical.it

² Dept. of Civil, Environmental and Architectural Engineering, Via Marzolo, 9, 35131 Padova, Italy; E-Mail:

vladimiro.achilli@unipd.it

³ Dept. of Informatics, Modeling, Electronic and System Engineering, University of Calabria, Via P. Bucci cubo 42C, 87036 Rende, Italy; E-Mail: raffaele.zinno@unical.it

* Correspondence: serena.artese@unical.it; Tel.: +39-0984-496768

Abstract:

Vertical displacements are among the most important technical parameters to evaluate the health status of a bridge structure and to verify its bearing capacity. Several methods, both conventional and innovative, are used for structural displacement monitoring; no one of these does allow, at the same time, precision, automation, long term and dynamic monitoring without using high cost instrumentation. The proposed system makes use of a common laser pointer and image processing. The measurement of the lowering is obtained by analyzing the single frames of a HD video of the laser beam imprint projected on a flat target. For the processing of images, a code was developed in Matlab® that provides the instantaneous displacement of a bridge, charged by a mobile load. An important feature is the synchronization of the load positioning, obtained by GNSS receiver or by a video. After the calibration procedures, a test was carried out during the movements of a heavy truck maneuvering on a bridge. Data acquisition synchronization allowed to relate the position of the truck on the deck to the displacements. The results show high accuracy and demonstrate that the method is suitable for dynamic load tests, ever more adopted for the bridge controls and monitoring.

Keywords: laser pointer, displacement monitoring, laser fingerprint, video, data synchronization.

1. Introduction

The possibility to perform fast and accurate image processing, thanks to the power of the most recent computers, allows us to conceive new exciting applications of this technology in several fields and, in particular, for monitoring large structures. The projection of the tangent to the elastic line of a girder, materialized by a light beam, on an image sensor or on a target can be effectively used for this aim. Nowadays this is possible in a cheap and simple way, thanks to the laser technology. Several laser pointers are presently available on the market, characterized by low cost, small dimensions and weight, low power, limited beam divergence and good pointing stability. All these characteristics allow the setup of a technique for monitoring large structures and in particular bridges.

Vertical displacements are among the most relevant technical parameters for assessing the health status of a bridge structure and for checking its load capacity. This parameter is also used to verify if the structural response of a bridge under various loading conditions is the one foreseen in the design phase. To control the state of health of a bridge before the opening to traffic, the structure is usually charged by static loads, materialized by a convoy of heavy trucks parked on the deck in known positions. The deflections of the girders are then measured by using levels or total stations. The Italian Rules for Constructions NTC 2008, e.g., impose a load test for any new bridge. Static

tests, in relation to the importance of the work, can be supplemented by dynamic tests on structural elements [1].

Several methods, both conventional and innovative, are used for structural displacement monitoring; all of these have pros and cons. (1) Dial gauges, often-used for measurements of floor slabs deflections, are difficult to install and manage, due to the height of bridges and the presence of water; (2) Digital levels are characterized by high precision, but they cannot perform dynamic multitarget measurements; (3) Robotic total stations can perform 3D coordinates measurements with a sampling rate up to 7 Hz and for velocities up to about 10 cm/s [2-3]. The high precision and the automation of measurement can be joined to the possibility of data transfer over the internet and remote management [4], but the high cost of this high-end instruments limits their use for long-term bridge monitoring; (4) GNSS satellite-surveying are often used for long span bridges [5-7]. The attainable precision is high and the maximum sampling rate exceeds 20 Hz for the recent instruments. The main disadvantage is due to the mandatory antenna positioning on the point to measure; (5) Terrestrial laser scanning (TLS) is by now a consolidated technique for the surveying of the bridges under static conditions [8,9]. The comparison of scans acquired at different times, allows us to obtain, e.g., the deviations between corresponding points of the bridge surface in different situations (loads, temperature, etc.). With regard to dynamic monitoring, the high sampling rate of line scanners, used in Mobile Mapping Systems, can be exploited. In particular, the deflections of the superstructure of a bridge could be dynamically measured in near real time. One must consider that the best fitting line has in general an accuracy rather better than each single measured point, so the final result could reach a precision higher than that declared for the instrument used [8,11]; (6) Micro Electro-Mechanical Systems (MEMS) have been recently proposed for deflection measurement using inclination parameter measurements [12]. The results are affected by the high S/N ratio for dynamic tests; (7) Digital Image Correlation is a promising technique for bridge deflection measurements, also thanks to the increasing resolution of the last digital cameras [13-15].

The use of a laser beam for measuring deflections is by now a consolidated technique. A laser based displacement/deflection measurement system is described in [16]. In order to achieve a remote measurement, the laser beam of a digital level is collimated and directed to a detector array, which is attached to the remote object to be measured. The system is not suitable for long-term measurements, since the level and the array must be placed on the monitored object and these expensive instruments must be left unattended. Recently a conception of measuring devices using a laser diode and a CCD camera has been proposed for structural monitoring [17].

Among the several technologies used for structures dynamic displacement monitoring, the methods based on laser projection-sensing are increasingly used, thanks to the availability of low-cost hardware. In this context, a methodology able to conjugate high precision, low cost and easiness of use has been set up. The measurement of the lowering is obtained by the variation of the tangent to the elastic line, materialized by the laser beam generated by a pointer attached to the deck bridge structure, and projected on a screen located at an adequate distance, in order to amplify the movement of the laser fingerprint and to get, therefore, a remarkable result accuracy. A video of the oscillations of the laser footprint during the monitoring activities is acquired. By analyzing the single frames, the variable position of the laser footprint centroid gives information about the inclination changes and, consequently, about the dynamic deflections. The position of the dynamic load can be detected by a video and/or GNSS positioning. The synchronization of acquisitions is performed by using GPS time.

The method is characterized by: (1) Low cost; (2) Low weight and small size hardware; (3) Ease of installation; (4) High precision; (5) High frame rate (30 frames per second, upgradeable to 120 by using a common action camera).

A method for displacement monitoring by using a laser beam, a projection plate plane and a camera has been presented in [18]. The method described in the present paper differs mainly in the following aspects: (1) In our test, a common low-cost laser pointer, battery-powered, is used; (2) The lab tests described in [16], conducted on a bridge model, refer to loads in a fixed position, so the synchronization of load positioning and images capturing, that represents a fundamental topic for

dynamic monitoring, is not considered; (3) Our test has been performed on a real bridge, with a real mobile load.

In the following, the methodology for monitoring of dynamic displacement of a bridge by using a low-cost laser pointer is presented, characterized by low cost, ease of implementation and high precision. Another important characteristic of this methodology is the synchronization of the moving load position and the deflection measurement. The experimental test carried out on a real bridge demonstrates the usability of this method for dynamic structures monitoring.

This paper covers: (1) a description of the methodology; (2) the hardware components (laser pointer, digital cameras, GNSS receiver, computer); (3) the software implemented (determination of laser footprint, time registration, inclination and displacement measurement); (4) the calibration procedures; (5) the in-field test; (6) the discussion of results.

2. Materials and Methods

2.1 The methodology

The proposed method takes advantage of the laser pointers' property to provide a steady pointing direction and produce a long-range, high-brightness visible imprint.

The footprint of a laser positioned at the intrados of a beam and projected on a plane target approximately orthogonal to the direction of the ray, will undergo a displacement ΔH due to two components: (1) the lowering or raising of the laser source and (2) the variation of the laser beam inclination. Both components are linked to the movements and inclinations of the structure to which the laser source is locked (Figure 1). The component (1) produces a shift δ of the laser footprint equal to the displacement of the laser source. The component (2) causes a displacement αD proportional to the distance between the laser source and the target. It is therefore possible to greatly amplify this displacement by positioning the target at a convenient range; this allows to obtain the tilt variation with remarkable precision.

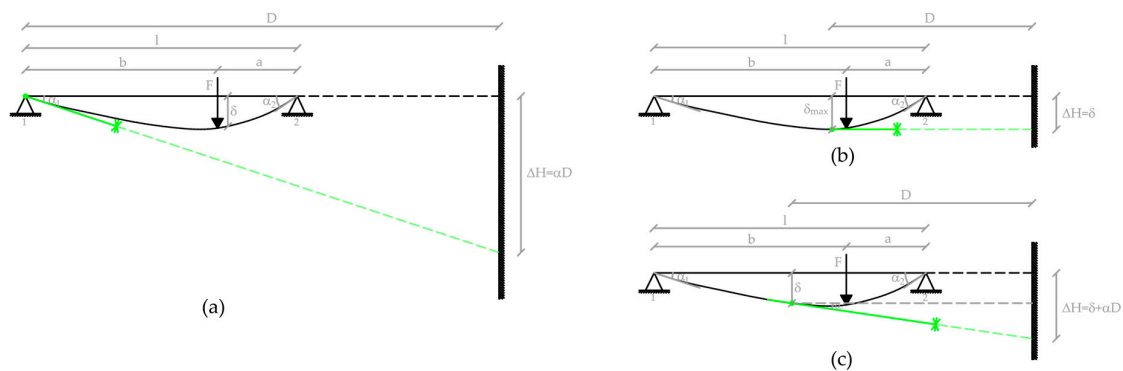


Figure 1. The displacement of the laser footprint in three cases: (a) laser fixed to a point subject only to inclination; (b) laser fixed to a point subject only to lowering; (c) laser fixed to a point with both inclination and lowering.

Lowering and inclination vary depending on the type of structure and the point of application of the load [19]. E.g., in the case of a point load applied to a simply supported uniform beam, the maximum displacement is given by:

$$\delta_{max} = \frac{Fa(l^2 - a^2)^{3/2}}{9\sqrt{3}EI} \quad (1)$$

This maximum deflection occurs at a distance x_1 from the closest support, given by:

$$x_1 = \sqrt{\frac{l^2 - a^2}{3}} \tag{2}$$

The slopes at the ends are:

$$\begin{aligned} \alpha_1 &= \frac{Fa(l^2 - a^2)}{6lEI} \\ \alpha_2 &= \frac{Fab(2l - a)}{6lEI} \end{aligned} \tag{3}$$

where:

- F = Force acting on the beam
- l = Length of the beam between the supports
- E = Modulus of Elasticity
- I = Area moment of Inertia of cross-section
- a = Distance from the load to the closest support (i.e. $a \leq l/2$)

the ratio between maximum deflection and slope at end 1 is given by:

$$\frac{\delta_{max}}{\alpha_1} = \frac{2\sqrt{(l^2 - a^2)}}{3\sqrt{3}} \tag{4}$$

the ratio between the deflection at the distance x from the end and the slope at end 1 is given by:

$$\frac{\delta_x}{\alpha_1} = \frac{x(l^2 - x^2 - a^2)}{(l^2 - a^2)} \tag{5}$$

By measuring the inclination at an extreme point where the laser pointer is fixed and knowing the point of application of a load, it is therefore possible to obtain the lowering of the span at any point. The measurement of the slope due to a load is obtained by the variation of the tangent to the elastic line, materialized by the laser beam projected by the pointer, fixed to the truss beam of the bridge, on a screen located at a suitable distance, in order to amplify the movement of the laser fingerprint and to get, therefore, a remarkable result accuracy. A video of the oscillations of the laser footprint is acquired; by analyzing the single frames, the variable position of the laser footprint centroid gives information about the slope changes and, consequently, about the dynamic deflections. The position of the dynamic load can be detected by a video and/or GNSS positioning. The synchronization of the acquisitions is performed by using GPS time. A first test was carried out on a bridge, whose structure is a simply supported space frame girder.

2.2 The hardware components

The hardware components are: (1) a laser pointer; (2) a digital camera for laser footprint video capturing and a camcorder for the video of the mobile load; (3) a GNSS receiver; (4) a computer with a synchronized clock.

2.2.1 The Laser Pointer

A SCITOWER SCT306-532nm laser pointer was used. The main characteristics are resumed in Table 1.

Table 1. Characteristics of the laser pointer.

Feature	Value
Wavelength	532 ± 0.1 nm (Green)
Beam diameter	2.0 mm
Beam divergence	0.8 mrad

Power	100 mW (Gaussian Beam)
Pointing stability	< 0.05 mrad
Beam spot roundness	$\geq 90 \%$
Laser distance	~ 500 m
Warm-up time	≤ 1 minute
Lifetime	≥ 8000 H

166
167 The laser pointer was mounted on a Newport Research Corporation model 810 laser mount,
168 provided with a strong magnetic base and two micrometric adjustment screws for a two axis
169 positioning.

170 2.2.2 The Digital Camera

171 The video of the laser footprint was acquired by using a NIKON D610 camera with a 55 mm
172 NIKKOR lens. The main characteristics are shown in Table 2.

173 **Table 2.** Characteristics of the NIKON D610 digital camera

Feature	Value
Type	Single-lens reflex digital camera
Effective pixels	24.3 million
Image sensor	Nikon FX format 35.9 x 24.0 mm - DX format 24x16 mm
File format	NEF (RAW), JPEG, NEF (RAW)+JPEG
Lens	NIKKOR 18-55mm f/3.5-5.6G VR
Shutter	Electronically-controlled vertical-travel focal-plane shutter
ISO sensitivity	ISO 100 to 6400 in steps of 1/3 or 1/2 EV
HD frame and frame rate	1,920 x 1,080 pixels; 30p (progressive), 25p, 24p

174
175 As for the video of the mobile load (a truck), a Canon Legria HF R78 Full HD Handycam was
176 used.

177 2.2.3 The GNSS Receiver

178 The GNSS receiver is an Ublox NEO-M8T provided with a cheap patch antenna. The NEO-M8T
179 is a timing receiver, but it can provide access to raw measurements on L1 (carrier-phase,
180 pseudorange, Doppler) for all available GNSS constellations and augmentation systems. For our
181 aims the receiver was configured to track GPS and GLONASS.

182 2.2.4 The Computer

183 A Dell XPS 13 9360 Notebook was used. The CPU is an Intel Core i7-7500U with a 2.7GHz clock
184 and 8 GB DDR SDRAM. The notebook is provided with a 256 GB SSD hard disk, a 13.3 inch Full HD
185 display and a graphic card Intel HD 620. The operating system is Windows 10 Pro. The
186 synchronization with *time.windows.com* can be performed with an accuracy of 1 ms. Time format was
187 set up in order to show hundredths of a second.

188 2.3 The software implemented

189 A program was developed in Matlab® for the determination of the laser footprint centroid
190 projected on a flat target. The program uses the results of the calibration of the digital camera,
191 described afterwards. With regard to the mean scale of the frame, the Ground Sample Distance
192 (GSD) is obtained at the beginning of the shoot, given that a millimeter paper glued to a rigid plastic
193 tablet is used as target. The millimeter paper allows to obtain the GSD, theoretically different for
194 each pixel, but it has to be considered that the target is fixed vertically and the camera optical axis is
195 horizontal, so the scale of the image in the vertical direction is practically identical in all the zones of
196 the frame.

197 To obtain the position of the laser footprint centroid, for each frame, an intensity cut-off is
198 performed preliminarily, in order to eliminate noises and the grid of the millimeter paper from the
199 image. The centroid coordinates (row and column) are then calculated in pixels, through a weighted
200 average: each pixel is assigned a weight equal to its intensity. The coordinates of centroid are
201 converted in mm, by using the known GSD.

202 If the camera settings provide a very low ISO sensitivity and a small diaphragm aperture, you
203 can get a better defined shape of the laser beam footprint and avoid image saturation in the center
204 zone of the footprint. This allows a more accurate determination of the centroid.

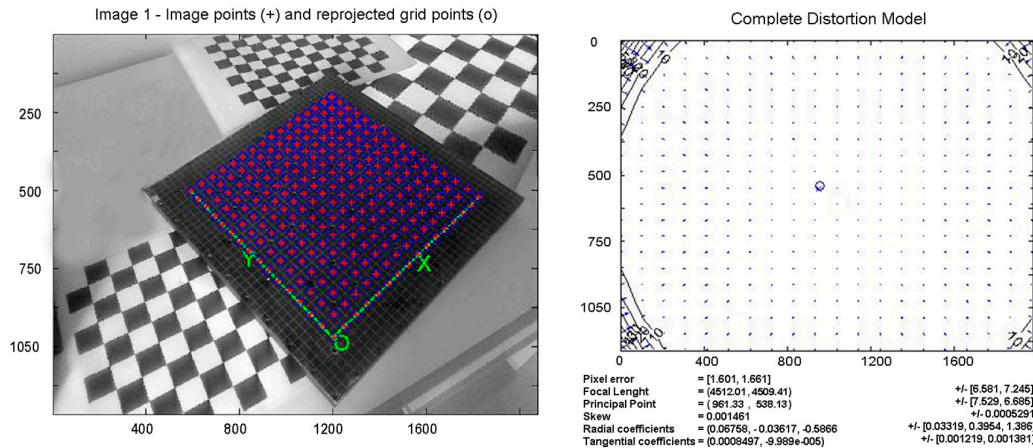
205 Given that the position of the centroid is given for each frame, it is possible to evaluate the
206 displacement of a monitored point with a sampling rate of 30 Hz. Thus we obtain a graph of the
207 centroid position as a function of time. Since the acquisitions of the video and of the mobile load
208 position are synchronized, the instantaneous displacement of the laser beam footprint is correlated
209 to the position of the mobile load.

210 A module of the implemented software is devoted to the calculation of the deflection. In the
211 first version, the laser pointer is considered fixed to an end of the bridge span; in this case the
212 deflection of the laser footprint is due just to the variation of the inclination of the laser beam, since
213 the end of the span has no deflection. The input of the module are: (1) the distance from the laser
214 pointer to the target; (2) the section inertia properties of the bridge; (3) the position of the mobile load
215 acquired by the GNSS receiver.

216 After the computation of the slope of the laser beam, the deflection is obtained for a requested
217 positions, e.g. for the midspan, by using equation (5). The procedure is performed for each frame of
218 the acquired video.

219 2.4 The calibration procedures

220 For the calibration of the camera, an upgrade of a well-known procedure [20,21], developed
221 using Matlab®, has been used. The procedure has been applied to the NIKON D610 camera with a
222 55 mm NIKKOR lens configured with a HD frame (1920 x 1080). A calibration plate with an accuracy
223 of .1 mm has been used. Figure 2a shows the points of intersection automatically recognized by the
224 software. If necessary, the operator can correct any errors or eliminate false positives identified by
225 the automatic procedure. The main parameters of the tested camera are shown in Figure 2b. The
226 results obtained are: focal length, principal point, skew, radial and tangential distortion parameters.

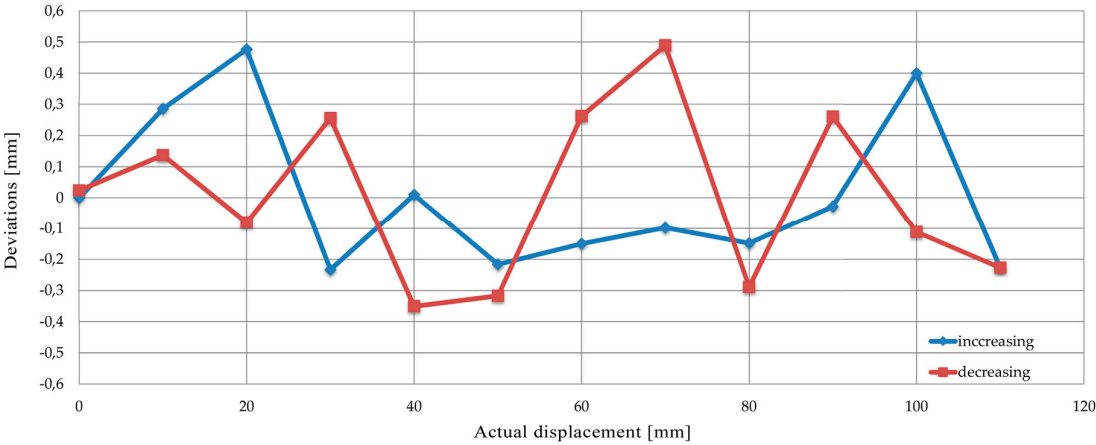


227 **Figure 2.** (a) The crosses of the calibration grid automatically recognized by the calibration
228 software; (b) The distortion model of the calibrated camera. The coordinates and the results are in
229 pixels.
230

231 After the camera calibration, to evaluate the accuracy of the centroid coordinates obtained by
232 the aforementioned software, a lab test was carried out. The laser pointer was fixed to a linear drive
233 unit Impex HVP060 AM, with a positioning precision 0.03 mm. The beam was projected
234

orthogonally on a flat target and the laser pointer was shifted 120 mm, with 2 mm steps. Shifting was applied many times back and forth, thus resulting in loop processes. In Figure 3 the deviations between the displacements obtained by the software and the ones produced by the linear drive unit are shown.

The horizontal axis represents the displacement of the laser source; the blue dotted line represents the deviations during the increasing displacements, whereas the red line represents the deviations during the decreasing ones. The maximum deviation is 0.5 mm, while the standard deviation is 0.25 mm.



243

244 **Figure 3.** The deviations between the displacements obtained by the software and the from the
245 displacements produced

246

247 To verify the laser pointer stability, the pointer and the target were positioned on the bridge to
248 be monitored, to have about the same environmental conditions of the test to be carried out.

249 Fifteen videos of five minutes were shot at an hour interval and, for each video, the oscillations
250 of the laser fingerprint centroid were obtained. The short term instability was almost negligible: in
251 fact, a maximum oscillation of 5 pixels during each video was measured, corresponding to an angle
252 of about 0.01 mrad, whereas the maximum difference measured in all videos was 14 pixels.

253

254 **3. The Test**

255 The test was carried out on the bridge of the University of Calabria, Italy. The University of
256 Calabria is characterized by a South-North axis, along which the buildings of the Departments are
257 sited. The axis is materialized by a sequence of double-deck bridges: the upper deck can be used for
258 vehicular traffic, while the lower one is reserved for pedestrians (Figure 4).

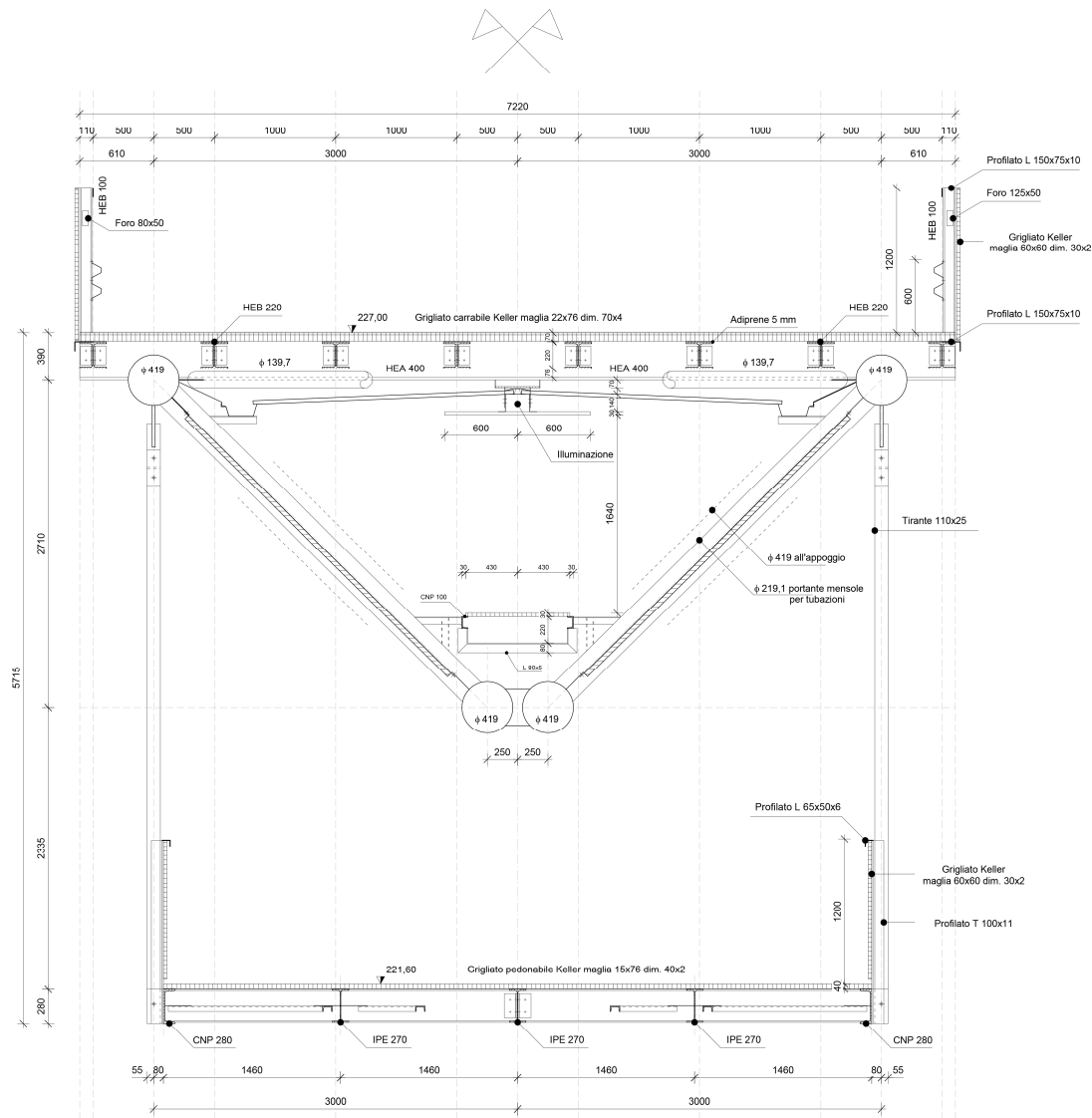


Figure 4: Cross section of the double-deck bridge at the University of Calabria.

The layout of the test is shown in figure 5. The laser pointer is fixed to a tubular element of the space frame girder of the bridge, close to the end of the span (Figure 6, 7). The laser beam is projected onto an A4 size flat target, fixed to a vertical wall of the north terminal abutment. To point exactly at the target, the pointer is mounted on a holder, usually used on optical tables, which allows precise horizontal and vertical movements. The holder is equipped with a strong magnetic base.

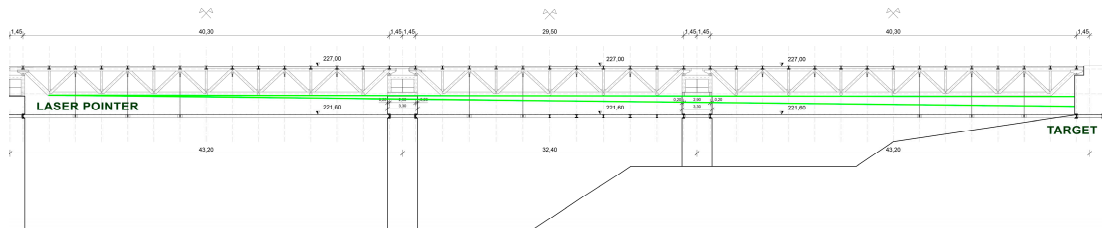


Figure 5 : The layout of the test.

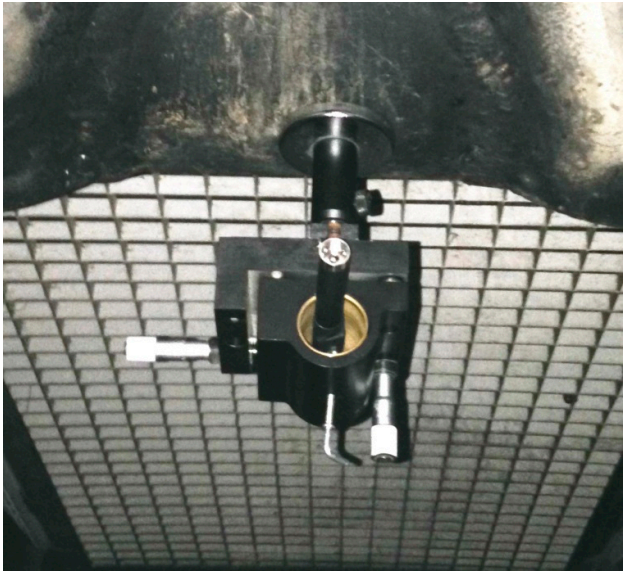


Figure 6 : The laser pointer and the holder.



Figure 7 : The pedestrian deck: the target is on the front wall.

269
270
271

272
273
274
275
276
277
278
279
280
281
282
283
284
285

The NIKON 610 camera, used to obtain the footprint video, is positioned on a robust tripod, slightly lateral respect to the laser beam path. The camera-target distance is chosen in order to obtain a Field of View (FoV) slightly larger than the dimensions of the target. Due to the camera-target distance and the lens focal length, the mean GSD is 0.25 mm. Taking into account the pointing stability of the laser pointer, a smaller GSD would be useless. Given that the distance from the laser pointer to the target is 115.70 m, we obtain a beam footprint diameter of 95 mm and a maximum theoretical pointing instability of 5.8 mm (23 pixels).

The projection plate plane and the optical path are not angled. Actually, by using e.g. a 30° angle like in [18], the movement of the laser spot centroid in the video image is amplified, and the measurement accuracy is theoretically increased, but this improvement is counterbalanced by the need to double the FoV and, consequently, the GSD.

286 The correlation techniques allow us to determine the centroid of the footprint with an accuracy
287 better than one pixel, thus the expected error in the measurements of the beam inclination is almost
288 completely due to the laser pointer instability and can be conservatively evaluated 0.05 mrad.

289 The test was carried out during the movements of a truck elevator, used for work on the façade
290 of a building alongside the bridge (Figure 8). The patch antenna of the Ublox NEO-M8T receiver was
291 positioned on the cab roof. The weight of the truck was about 260 kN. The video of the mobile load
292 was shot with the camcorder when the truck left the bridge. Due to the limited space, the truck
293 performed some forward and backward movements to reach the optimal alignment before the final
294 reverse running.

295 With regard to time synchronization, the Nikon 610 camera is provided with a GP-1 unit, an
296 accessory that can provide the Coordinated Universal Time (UTC). For the synchronization of the
297 camcorder, the display of the notebook, showing the GPS time rounded to the hundredths of a
298 second, was framed before and after the video shot. In this way, the video's timing synchronization
299 was obtained with an approximation equal to its frame rate of 30 fps.
300



301
302

Figure 8: The truck elevator on the upper deck of the bridge.

303
304

305 A frame of the video is shown in Figure 9. The image shows the truck during the backward
306 running. The transverse beams of the upper deck, positioned every three meters, allow to determine
307 the position of the wheels in the longitudinal direction. The origin of abscissae (positive in North
308 direction) is fixed at the south end of the span.

309 The accurate abscissae of the truck were obtained by a cinematic differential positioning. The
310 Ublox GNSS receiver was set to acquire data with a 5 Hz sampling rate, while the fixed GNSS station
311 at University of Calabria was used as base. Furthermore, two points on transverse beams of the
312 upper deck were surveyed previously, in order to perform a coordinate transformation and obtain
313 the abscissae in the local reference system.
314



Figure 9: A frame of the camcorder video with the truck leaving the bridge. The transverse beams on the deck are used to obtain the position in the direction parallel to the longitudinal axis of the bridge.

4. Results and Discussion

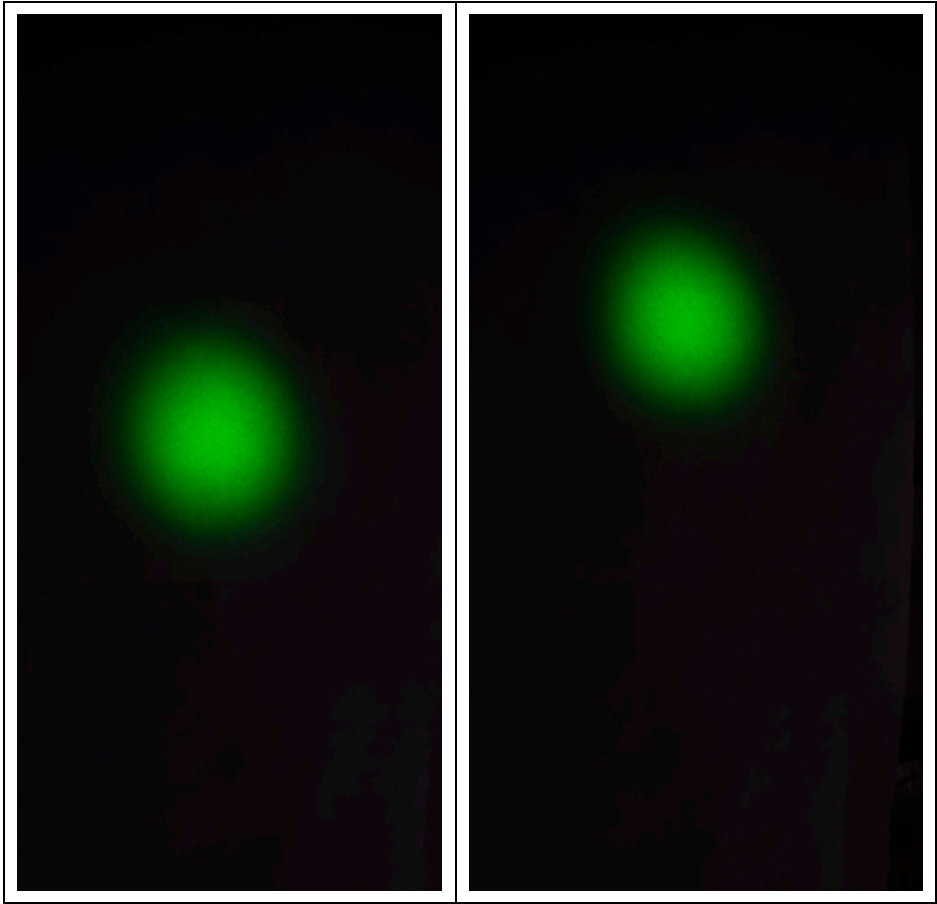


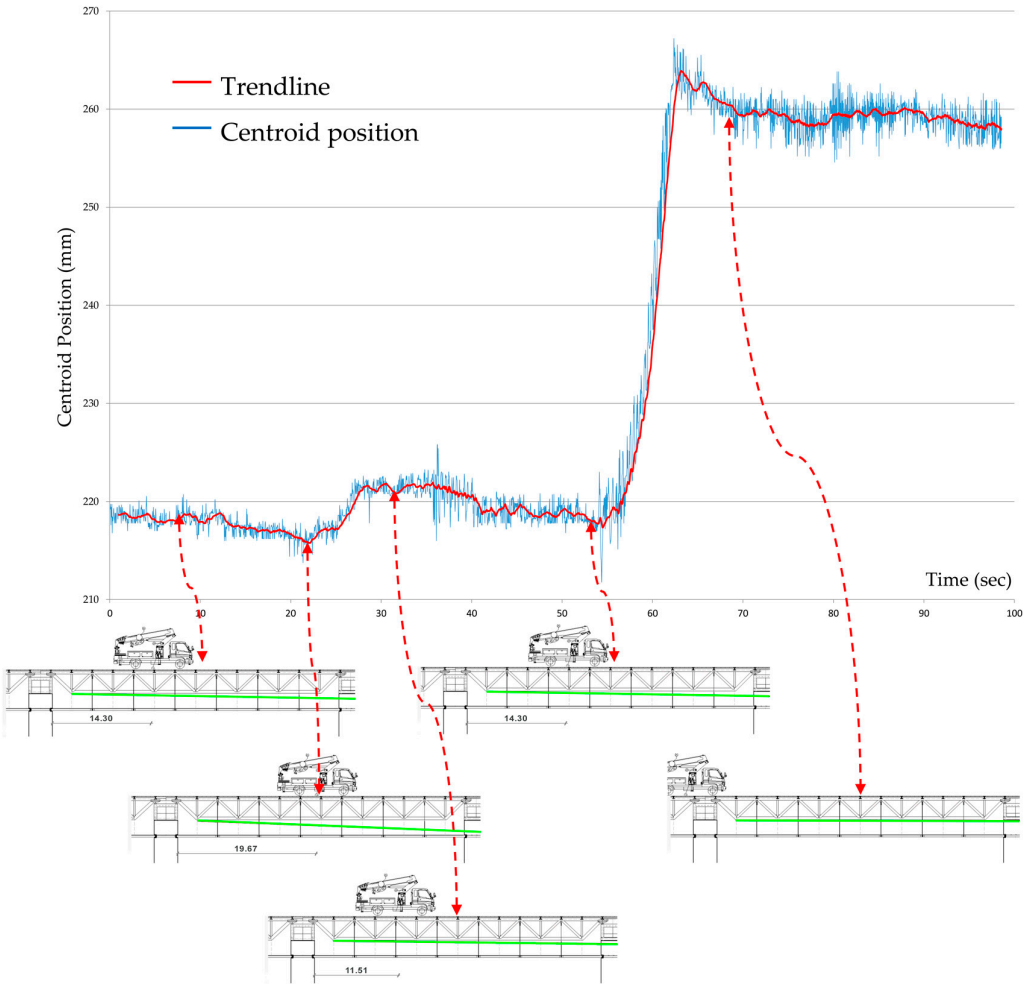
Figure 10: two frames acquired at the beginning and at the end of the test: after the truck left the bridge, the footprint is higher.

323 In the Figure 10 we can observe two frames obtained at the beginning and at the end of the test.
324 The ISO sensitivity and the aperture were chosen in order to obtain a radiometric cut off, thus
325 achieving two goals: a better defined shape of the laser beam footprint was obtained and the
326 saturation of the image in the center zone of the footprint avoided. This allows a more accurate
327 determination of the centroid. The frames were processed by using the code in Matlab® previously
328 described and the dynamic position of the centroids in pixel coordinates (rows, columns) was
329 obtained.

330 In Figure 11 , the height of the centroid during the test is shown. In red a trend line (30-sample
331 moving average) is drawn. The origin of ordinates is at the bottom of the frame and the values have
332 been transformed from pixels into mm, while the scale of the frames has been obtained by using the
333 known GSD. Abscissae are in seconds.

334 It is possible to observe that the pointing stability was less than 0.05 mrad (corresponding to 5.8
335 mm for the pointer–target distance equal to 115.70 m).

336 From a qualitative point of view we can observe that the forward – backward movements of the
337 truck are clearly reflected in the movements of the laser beam. Furthermore, some damped
338 oscillations are recognizable after the truck left the bridge.
339



340
341

342 Figure 11: The vertical position of the centroid of the footprint during the test.
343

As regards the truck position, the abscissae obtained by using the GNSS positioning were used for the elaborations. A comparison between the abscissae obtained by the camcorder video and by the GNSS solution showed a maximum deviation of 0.3 m.

The span of the bridge is 40.30 m, while the barycenter of the truck, at the beginning of the test, is at 14.30 m from the bearing.

After 55 seconds from the beginning of the video, a sudden variation is evident, equal to about 40 mm, corresponding to an inclination change of 0.346 mrad. Given that the laser is positioned very close to the bearing and the section inertia properties of the truss beam are constant, the estimation of the maximum deflection can be made by using equation (4). The variation of the truss beam deflection obtained this way is 5.0 mm. The variation of the deflection in the midspan, obtained by using equation (5), is 4.9 mm.

A precise measurement was done by using a Leica 1201+ total station. The axis of a bolt of a steel connection in the midspan was used as a target and its position was surveyed before and after the test. The measured variation of the truss beam deflection was 4.8 mm, 2% less than the result obtained with the proposed methodology.

The use of the positions obtained by the camcorder video and by the GNSS solution gave results comparable, with differences less than 5%. Both techniques have pros and cons. GNSS allows to obtain more accurate positioning along with a simple and accurate time synchronization, but a receiver must be installed on the vehicle. The video gives less accurate positioning, implies more computer processing both for images and time synchronization, but it can be used also for not instrumented vehicles. For official load tests, the first technique is the most suitable; in fact, in order to obtain the requested precision of positioning, the vehicles used as mobile loads can be easily provided with a GNSS receiver. For the monitoring of a bridge under normal conditions, instead, the second technique is the only currently usable.

5. Conclusions

In the light of the results of the test carried out on a real case, we can conclude that the method proposed allows to obtain the deflections of a bridge with the precision required for load tests and monitoring. The low cost of the components and the ease of configuration make the method a suitable alternative to the traditional methods. Its reliability has been demonstrated both from a qualitative and quantitative point of view. The forward – backward movements of the truck used for the experimental test are clearly reflected in the movements of the laser beam. The deviation between the beam deflection obtained with the described method and the one measured by a high-end total station was about 2%.

Along with the precision obtained, a noticeable goal is the synchronization of the acquisitions, that allows to get the instantaneous position of the mobile load and the deflection.

In the next future, the use of a camera with high frame rate is foreseen, in order to demonstrate the usefulness of the method for the control of the bridge's natural frequencies.

Author Contributions: Serena Artese conceived the methodology. Serena Artese and Vladimiro Achilli designed the experiments. Raffaele Zinno analyzed the data. All the authors performed the experiments and prepared the manuscript.

Conflicts of Interest: The authors declare no conflict of interest.

References

1. Italian Ministry of Infrastructures and Transportations. NTC (2008). Norme Tecniche per le Costruzioni, Ministerial Decree 14/01/2008, Official Gazette n. 29, Rome, Italy, 2008.
2. Lienhart, W.; Ehrhart, M.; Grick, M. High frequent total station measurements for the monitoring of bridge vibrations. *Journal of Applied Geodesy* **2017**, *11*, 1-8, doi: 10.1515/jag-2016-0028
3. Yu, J.; Zhu, P.; Xu, B.; & Meng, X. Experimental assessment of high sampling-rate robotic total station for monitoring bridge dynamic responses. *Measurement* **2017**, *104*, 60-69, doi: 10.1016/j.measurement.2017.03.014

4. Artese, G.; Perrelli, M.; Artese, S.; Manieri, F. Geomatics activities for monitoring the large landslide of Maierato, Italy. *Applied Geomatics* **2014**, *7*, 171-188, doi: 10.1007/s12518-014-0146-8.
5. Lovse, J. W.; Teskey, W. F.; Lachapelle, G.; & Cannon, M. E. Dynamic deformation monitoring of tall structure using GPS technology. *Journal of surveying engineering* **1995**, *121*(1), 35-40, doi: 10.1061/(ASCE)0733-9453(1995)121:1(35).
6. Roberts, G.; Meng, X.; Dodson, A. Integrating a Global Positioning System and Accelerometers to Monitor the Deflection of Bridges. *Journal of Surveying Engineering* **2004**, *130*, 65-72, doi: 10.1061/(ASCE)0733-9453(2004)130:2(65).
7. Yu, J.; Meng, X.; Shao, X.; Yan, B.; Yang, L. Identification of dynamic displacements and modal frequencies of a medium-span suspension bridge using multimode GNSS processing. *Engineering Structures* **2014**, *81*, 432-443, doi: 10.1016/j.engstruct.2014.10.010.
8. Gordon, S.; Lichti, D. Modeling Terrestrial Laser Scanner Data for Precise Structural Deformation Measurement. *Journal of Surveying Engineering* **2007**, *133*, 72-80, doi: 10.1061/(ASCE)0733-9453(2007)133:2(72).
9. Park, H. S.; Lee, H. M.; Adeli, H.; & Lee, I. A new approach for health monitoring of structures: terrestrial laser scanning. *Computer-Aided Civil and Infrastructure Engineering* **2007**, *22*(1), 19-30, doi: 10.1111/j.1467-8667.2006.00466.x.
10. Truong-Hong, L.; Laefer, D. F. Using Terrestrial Laser Scanning for Dynamic Bridge Deflection Measurement, Proceedings of the IABSE Istanbul Bridge Conference, Istanbul, Turkey, 11-13 August 2014.
11. Artese, S. Survey, diagnosis and monitoring of structures and land using geomatics techniques: theoretical and experimental aspects. In *Geomatics research 2016*, Vettore, A., Ed.; AUTeC, Italy, 2017; pp. 31-42, ISBN 978-88-905917-9-2.
12. Yu, Y.; Liu, H.; Li, D.; Mao, X.; & Ou, J. Bridge deflection measurement using wireless mems inclination sensor systems. *International Journal on Smart Sensing & Intelligent Systems* **2013**, *6*(1), 38-57, doi: 10.1.1.658.8791.
13. Yoneyama, S.; Ueda, H. Bridge deflection measurement using digital image correlation with camera movement correction. *Materials Transactions* **2012**, *53*(2), 285-290, doi: 10.2320/matertrans.I-M2011843.
14. Kwak, E.; Detchev, I.; Habib, A.; El-Badry, M.; Hughes, C. Precise photogrammetric reconstruction using model-based image fitting for 3D beam deformation monitoring. *Journal of Surveying Engineering* **2013**, *139*(3), doi: 143-155, 10.1061/(ASCE)SU.1943-5428.0000105.
15. Lu, W.; Cui, Y.; Teng, J. Structural displacement and strain monitoring based on the edge detection operator. *Advances in Structural Engineering* **2016**, *20*, 191-201, doi: 10.1177/1369433216660220.
16. Tang, C.; Li, E. The design of a laser-based digital displacement/deflection measurement system of a remote object and its calibration. *Proc. SPIE 6829, Advanced Materials and Devices for Sensing and Imaging III*, 68291T (24 January 2008); doi: 10.1117/12.757617.
17. Wilczyńska, I.; & Ćmielewski, K. Modern measurements techniques in structural monitoring on example of ceiling beams. Proceedings of 3rd Joint International Symposium on Deformation Monitoring (JISDM), Vienna, Austria, 30 March - 1 April 2017.
18. Zhao, X.; Liu, H.; Yu, Y.; Xu, X.; Hu, W.; Li, M.; Ou, J. Bridge displacement monitoring method based on laser projection-sensing technology. *Sensors* **2015**, *15*(4), 8444-8463, doi: 10.3390/s150408444.
19. Chen, W.; Lui, E. *Handbook of structural engineering*, 2nd ed.; CRC Press: Boca Raton, United States, 2005; pp 1768, ISBN: 9780849315695.
20. Zhang, Z. A flexible new technique for camera calibration. *IEEE Transactions on Pattern Analysis and Machine Intelligence* **2000**, *22*, 1330-1334, doi: 10.1109/34.888718.
21. Artese, G.; Perrelli, M.; Artese, S.; Meduri, S.; Brogno, N. POIS, a Low Cost Tilt and Position Sensor: Design and First Tests. *Sensors* **2015**, *15*, 10806-10824, doi: 10.3390/s150510806.